Determining the dependence of marine pile driving sound levels on strike energy, pile penetration, and propagation effects using a linear mixed model based on damped cylindrical spreading

S. Bruce Martin[a] and David R. Barclay
Department of Oceanography, Dalhousie University, 1355 Oxford Street, P.O. Box 15000, Halifax, Nova Scotia, B3H 4R2, Canada

(Received 2 January 2019; revised 3 June 2019; accepted 5 June 2019; published online 11 July 2019)

Acoustic recordings were made during the installation of four offshore wind turbines at the Block Island Wind Farm, Rhode Island, USA. The turbine foundations have four legs inclined inward in a pyramidal configuration. Four bottom mounted acoustic recorders measured received sound levels at distances of 541–9067 m during 24 pile driving events. Linear mixed models based on damped cylindrical spreading were used to analyze the data. The model's random effects coefficients represented useful information about variability in the acoustic propagation conditions. The received sound levels were dependent on the angle between pile and seabed, strike energy, and pile penetration (PP). Deeper PPs increased sound levels in a frequency dependent manner. The estimated area around the piles where auditory injury and disturbance to marine life could occur were not circular and changed by up to an order of magnitude between the lowest and highest sound level cases. The study extends earlier results showing a linear relationship between the peak sound pressure level and per-strike sound exposure level. Recommendations are made for how to collect and analyze pile driving data. The results will inform regulatory mitigations of the effects of pile driving sound on marine life, and contribute to developing improved pile driving source models.
 https://doi.org/10.1121/1.5114797

[ANP] Pages: 109–121

I. INTRODUCTION

Offshore wind farms are being installed around the world to provide a sustainable source of electricity. In waters up to 50 m deep, wind turbines are normally secured to the seabed using impact pile driving, which generates intense impulses of sound that may disturb marine life 70 km from their source (Bailey *et al.*, 2010). This sound could have significant ecological effects on marine life. Pile driving sounds are often studied during the installation of wind farms (e.g., Madsen *et al.*, 2006; Betke, 2008; Matuschek and Betke, 2009; Bailey *et al.*, 2010; Brandt *et al.*, 2011; Dähne *et al.*, 2013; Wilkes and Gavrilov, 2017). The studies have demonstrated fish mortality at close ranges to the pile driving and temporary threshold shifts in fish hearing at longer ranges (Halvorsen *et al.*, 2011, 2012; Casper *et al.*, 2013; Casper *et al.*, 2017). Harbor porpoise have been shown to avoid pile driving at distances of 20 km or longer (Dähne *et al.*, 2013; Tougaard *et al.*, 2015) and exposure to intense impulsive sound can induce temporary threshold shifts in marine mammals (e.g., Finneran *et al.*, 2002; Lucke *et al.*, 2009; Finneran *et al.*, 2011; Kastelein *et al.*, 2017). Over the past two decades, American regulatory thresholds to minimize harm have been proposed for marine mammals (NMFS and NOAA, 1995; NOAA, 2013; NOAA, 2015; NMFS, 2016; NMFS, 2018) as well as fishes, turtles, and marine invertebrates (FHWG, 2008; Popper *et al.*, 2014). Erbe (2013) and Lucke *et al.* (2014) document underwater noise regulations developed in many other jurisdictions. Despite this progress many questions remain about which properties of a sound determines its impact on different marine taxa, for example, amplitude, energy, rise time, and repetition rate all contribute to a sound's effects (Finneran, 2015; Popper *et al.*, 2019). New results continue to emerge that better describe the generation and propagation of sound from pile driving (Newhall *et al.*, 2016; Dahl and Dall'Osto, 2017; Wilkes and Gavrilov, 2017; Lippert *et al.*, 2018).

When an impact hammer strikes the top of a pile, the Poisson effect creates a compressional deformation that propagates down the pile as a band of increased diameter at speeds on the order of 5000 m/s. When the deformation enters the water, it creates an acoustic pressure wave that propagates at the sound speed in water, ~1500 m/s. The difference in sound speed between the metal pile and the water creates a Mach cone angled 15–19 deg from the axis of the pile (Dahl, 2015; MacGillivray, 2018). The Mach cone acts as a continuous line source of sound rather than of a point source. Sophisticated methods are required to predict and accurately measure the sound signatures, especially within three water depths of the pile (Reinhall and Dahl, 2011; Ainslie *et al.*, 2014). At distances greater than three water depths the received sound exposure level (SEL) is expected to follow

$$L_E(R) = \text{constant} - (A \log_{10} R + BR), \quad (1)$$

where R is the range from pile to receiver in meters, the constant is the regression's intercept term that fits the data, A is

[a]Also at JASCO Applied Sciences Canada, Suite 202, 32 Troop Avenue, Dartmouth, NS, B3B 1Z1. Electronic mail: bruce.martin@jasco.com

in the range of 10–20, and B arises from multiple reflections of the sound from the seabed and surface (Zampolli *et al.*, 2013; Ainslie *et al.*, 2014; Lippert *et al.*, 2018). The propagation parameters A and B depend on the bottom composition, the water column sound speed profile, as well as the surface and seabed roughness. Equation (1) is a simple model that does not consider variations in bathymetry and bottom composition; however, it is useful for developing a conceptual understanding of pile driving sound propagation and as a framework for regression analysis of measured data (Ainslie *et al.*, 2014; Lippert *et al.*, 2018).

It is important to note that the constant in Eq. (1) is not a source factor but does depend on project specific conditions such as the hammer strike energy (SE), the coupling of the hammer energy into the pile, and the damping of pile vibrations by the sediment surrounding the embedded end of the pile (MacGillivray, 2014; Lippert *et al.*, 2016). Previous measurements of the relationship between radiated sound levels and SE found a 10 dB increase in peak-to-peak sound pressure level (SPL) when SE increased from 63 kJ to 184 kJ (Bailey *et al.*, 2010), or a 12 dB increase in peak-to-peak SPL and an 8 dB increase in SEL for a 10 dB increase in SE (Robinson *et al.*, 2007). The peak SPL attenuates more quickly with range than SEL due to dispersive effects in shallow water, as well as interactions with the sea-surface and seabed, which scatters high frequencies. Therefore, recordings at different ranges likely would have changed the measured relationship between SE and peak-to-peak SPLs (Lippert *et al.*, 2015).

The Block Island Wind Farm is the first offshore wind farm installed in the United States. It is located ∼6 km from Block Island, RI. The farm has five 6 MW turbines. Each turbine is mounted on four-leg-jacket foundations pinned to the seabed with ∼60 m long, 1.52 m diameter piles that were driven in three sections. The foundation legs were identified as A1, A2, B1, and B2, while the piles sections were identified as P1, P2, and P3. The piles were aligned with the cardinal points of the compass and inclined ∼14-deg inward so that the foundation is like a pyramid. The leg inclination of ∼14 deg is similar to the Mach cone angle, so that the Mach cone on the outside of the pile should propagate with fewer bottom and surface interactions than the cone inside the pile. This suggests that the acoustic propagation losses could have a directional component. A similar pile configuration was measured by Bailey *et al.* (2010) where significantly different peak-to-peak SPLs were measured on one side of the pile compared to the other. Bailey *et al.* (2010) propose that this could be due to different tidal conditions or bathymetry effects, and suggest that a long-term static recording program at multiple ranges from multiple piles would be needed to determine the cause of these differences. Wilkes and Gavrilov (2017) modeled and measured inclined (raked) piles in shallow water (7 m) and confirmed that there is directional variability in the received sound levels.

The Block Island project's incident harassment authorization[1] and United States Army Corps of Engineers permit[1] included acoustic thresholds for biological effects of sound on marine life and estimates of the distance from the piles that sound levels were above the thresholds (Table I). A conceptual line drawn on a map that joins points with equal sound levels is called an isopleth. The project team was required to maintain a visual watch for marine mammals within the 600 m level A isopleth and to shut down piling if a mammal was present. The isopleth distances estimated during the permitting process (Table I) were based on the practical spreading model (NOAA, 2012), which does not include any location specific information that would affect sound propagation. As a result, the monitoring conditions in the Block Island Wind Farm permit required a systematic sound source characterization study. The study included short- and long-term components. The short-term study used real-time acoustic measurements from a vessel as well as sound levels measured at four or five ranges using bottom mounted recorders. The recorders were retrieved each evening, the data downloaded and analyzed by linear regression [using Eq. (1)] to estimate isopleth radii that were assumed to be circular. Twelve pile sections were analyzed during the short-term monitoring from 30 Aug to 18 Sept 2015. The long-term study used bottom mounted recorders to measure ambient sound levels and pile driving of 24 pile sections in September and October, 2015.

TABLE I. Permitted sound level isopleths for impact pile driving at the Block Island Wind Farm.[1] The distances were estimated by National Marine Fisheries Service (NMFS) assuming an attenuation of $15\log_{10}(R)$. For the 187 dB re 1 μPa^2 s $L_{E,24h}$ isopleth, a source factor of 219 dB re 1 μPa^{2}m^2 and a pile driving time of 27000 s was assumed.[2] The actual number of strikes ranged from 1960 (26 Oct) to 7812 (18 Sept).

Sound level threshold	Maximum radius (m)
206 dB re 1 μPa $L_{p,pk}$ (fish Injury)	7
180 dB re 1 μPa L_p (Level A marine mammal harassment)	600
166 dB re 1 μPa L_p (sea turtle disturbance)	3414
160 dB re 1 μPa L_p (marine mammal level B disturbance)	7000
150 dB re 1 μPa L_p (Fish Disturbance)	39 810
187 dB re 1 μPa^2 s $L_{E,24h}$ (Fish Injury)	116 591

A more detailed analysis of the short- and long-term data investigated methods for rapidly computing the pile driving sound regulatory isopleths (Martin *et al.*, 2016). The study compared three methods. The first two methods were straightforward. First, the data were fit to Eq. (1), and second the practical spreading model (NOAA, 2012) was applied at three different ranges. The third method was measured-modeled fit between the collected data and an ensemble of acoustic propagation models. For the measured-modeled fit, the pile was assumed to be a point source (to simplify the analysis) and a range of possible seabed geoacoustic properties were modeled. A minimum least squared fit was then performed to select the geoacoustic properties and source factor that minimized the difference between the data and model. All three types of analysis were applied to single pile driving events and produced an unsatisfactorily wide range of isopleth distances when compared across events and methods. For example, the methods produced ranges to the 160 dB re 1 μPa SPL isopleth between 3457 m and 7454 m for the same pile driving event (Martin *et al.*, 2016). As an

example of variability between events, the 160 dB re 1 μPa isopleth for the first segments of the four legs of foundation 3 were between 2011 and 4578 m (measured Aug. 30–Sept. 2, 2015).

Three questions arose from these analyses of the Block Island data: (1) what is the source of the large variability in sound levels between pile driving events?; (2) how does the variability affect the dimensions of biological effects isopleths?; and (3) given this variability exists, how should acoustic measurements and analysis be performed to accurately determine the radius around a piling event where the sound may affect marine life?

This study analyzes the received sound levels from 24 pile sections using a linear mixed model. The model included range, the angle between the pile and seabed, the SE and pile penetration (PP) as fixed effects, and allowed propagation variations due to pile-to-recorder bathymetry, bottom properties, and the sound speed profile to be represented by random effects. This structure separated the propagation effects from variability in the source sound levels. The model was used to predict the ranges to the sound isopleths. Two methods of estimating the isopleth prediction intervals were investigated. The paper is organized as follows. Section II describes the acoustic measurements and data analysis methods. Section III provides an overview of the measured pile driving sound levels, the linear model parameters, and the isopleth distances predicted by the model. Section IV discusses the isopleth distances and their variability, compares the current and previous results, and makes recommendations for future pile measurements and analysis.

Supplemental material[3] provides: (1) details of the recorder configurations and locations; (2) details of the Teager-Kaiser impulse detector; (3) pile locations and the 24 pile driving events analyzed; (4) typical data from all recorders for a single pile; (5) measured sound speed profiles; (6) examples of the pile driving logs; (7) further details on the performance of the linear models; (8) isopleth radii for the Block Island Wind Farm pile driving using a wide selection of regulatory thresholds; and (9) the outline for "***R***"-code to perform the linear mixed modeling and prediction interval estimation.

II. METHODS

A. Acoustic measurements

Continuous acoustic measurements sampled at 64 kHz were made using AMAR acoustic recorders (JASCO Applied Sciences, Dartmouth, NS) located the seabed at four ranges from the wind turbine foundations (Fig. 1). The sound intensity spreads throughout the water column and usually decreases at a rate between $1/R$ $(10\log_{10}R)$ and $1/R^2$ $(20\log_{10}R)$ (where R is the distance between the pile and receiver; Ainslie *et al.*, 2014). Since the intensity changes as the logarithm of the distance, the measurement locations were also spaced approximately logarithmically. The prediction intervals of linear models are smallest if the prediction range is inside the measured range. Therefore, it is desirable to put the recorder closest to the pile inside the shortest expected isopleth distance, and the farthest recorder outside the longest expected isopleth. The closest distance the

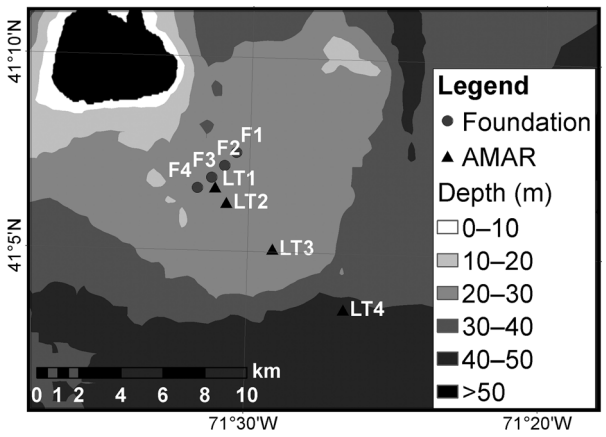

FIG. 1. Location of the four Block Island Wind Farm foundations (F1–F4) monitored in this study and the recorder locations (LT1–LT4). Foundation F5 (not shown) was completed during the short-term monitoring phase of the project.

recorders were permitted, for safety and logistical reasons, was 500 m. Since it was logistically impractical to deploy and retrieve recorders more than 10 km from the measurement site (the fish disturbance isopleth was 40 km; see Table I), the longest range was selected to be 9000 m and therefore recorders were placed at nominal ranges of 500, 1500, 4500, and 9000 m from foundation 3 (Fig. 1). The combination of pile driving events, as well as recorder and pile locations, resulted in 16 measurement ranges, of which 10 were approximately evenly distributed between 541 and 2550 m, 3 were around 4800 m, and 3 were near 9000 m.

Data from 80 pile and recorder combinations were analyzed spread across the 4 recorders and 24 piling events. Each pile leg (A1, A2, B1, and B2) was measured six times. All three pile sections were measured at foundation F1, as well as foundation F2, section 1; foundation F3, section 2; and foundation F4, section 3.

B. Acoustic data analysis

Data were provided by the pile driving contractor for the SE for every piling blow and the number of strikes required to penetrate each meter of sediment. To determine how sound levels varied with SE and PP, the sound levels for each pile impulse were required. The impulses were extracted from the raw acoustic data using a Teager-Kaiser (Kandia and Stylianou, 2006) energy detector with an averaging window set to 31 ms. For a subset of the pile strikes, the detector identified multi-path arrivals after the main impulse. To automatically remove the unwanted detections, they were grouped using K-means clustering with three clusters for (1) spurious high amplitude events, (2) the main group of events, and (3) the low amplitude multi-path arrivals (custom Python software, The Python Software Foundation,[4] V3.5.2) using the package "pyclustering" V0.6.6). The multi-path arrival cluster was set to have a mean SEL at least 12 dB below the main arrival group. Any events with higher SEL were included in the analysis.

For each impulse, the 0.125 s time window containing the highest squared pressure was selected for computing the

peak SPL ($L_{p,\mathrm{pk}}$), SPL, ($L_{p,\mathrm{rms.0.125s}}$), per-pulse SEL, ($L_{E,0.125\mathrm{s}}$), as well as the SEL in each decidecade band from 10 to 25000 Hz ($L_{E,0.125\mathrm{s,ddec}}$; terminology and metrics from ISO (2017) are used in this analysis). The fixed time window was selected to generate stable and reproducible SPL estimates. The duration of 0.125 s was chosen to be approximately as long as marine mammal auditory integration times (see Erbe *et al.*, 2016, for a discussion of auditory integration times). This duration was also a good match to the duration of the received pulses—75% of the pulses had a 90% energy duration less than 0.125 s. This window duration was also chosen because the 0.125 s duration leaky integrator ($L_{\mathrm{eq\text{-}fast}}$) has been shown to be well suited to the study of the effects of noise on marine mammals (Tougaard *et al.*, 2015). $L_{\mathrm{eq\text{-}fast}}$ is the fast-time weighted root-mean-square SPL defined for sound level meters (ANSI, 2006) that time-weights the received impulse so that the center 0.125 s of sound, as well as the following ~0.5 s, are summed in a manner similar to the measured response of human hearing (Tougaard and Beedholm, 2019). For this study, a 0.125 s fixed window rather than $L_{\mathrm{eq\text{-}fast}}$ was used since it is simpler to compute and therefore simpler to adopt as a recommended approach for analyzing pile driving data. The fixed window duration SPL is always greater than $L_{\mathrm{eq\text{-}fast}}$; it is 2 dB higher than $L_{\mathrm{eq\text{-}fast}}$ at 0.125 s duration for the actual pulse, and 4 dB higher for a 0.0625 s pulse [to verify this evaluate Eq. (1) of Tougaard *et al.*, 2015, for a range of actual pulse durations]. Thus, the fixed window duration is conservative in that it computes higher SPLs for short pulses that are closer to the 90% duration SPLs but does not excessively attenuate the SPL for longer pulses.

The technical guidance on effects of noise on marine mammals from the United States National Marine Fisheries Service recommends the peak SPL and auditory frequency weighted SEL as indicators of possible auditory injury or impairment (NMFS, 2018; Southall *et al.*, 2019; the auditory frequency-weighting names from Southall *et al.* are used here). Therefore, we have also computed auditory frequency weighted SELs from the 0.125 s window decidecade data. To verify that energy was not missed, the total SEL over the period of each pile driving event computed from the continuous data stream (which includes energy not associated with the impulses) was compared to the total SEL from just the detected impulses. The continuous SEL was within 1–2 dB of the energy contained in the impulses, even at the longest-range recorder (9067 m). The differences were smaller for the weighted SEL than the total SEL. The 10 Hz and above decidecades were summed to provide the broadband per-strike SEL ($L_{E,0.125\mathrm{s}}$). The per-strike SEL were summed to obtain the per-pile SEL.

C. Linear regressions

Regression analysis modeled the measured data so that estimates of the sound levels near the pile could be computed as a function of location and pile driving parameters. Predictor variables to describe the pile driving source were: the SE, the PP versus strike number, as well as the angle between the pile and the seabed along the line between each pile and recorder. SE and PP logs were provided by the construction contractor, Weeks, via Tetra Tech (Boston, MA) and Deepwater Wind (Providence, RI). The logs were digitized and time-aligned with the strike detection data. A measure of pile angle was needed. The foundation legs were oriented north-south/east-west, and recorders were deployed along a line extending to the southeast from foundation F3 (Fig. 1). The analysis variable $\theta_{\mathrm{Pile\text{-}Rec}}$ (pile - recorder angle) has a value of zero when the pile is inclined away from the recorder and a value of 180 when the pile is inclined toward the recorder. Its value was calculated from the angle between the foundation and the recorder plus the orientation of each pile leg.

Lippert *et al.* (2018) argued that sound levels from a pile should be modeled as damped cylindrical spreading (DCS), i.e., parameter A in Eq. (1) should be ten, and parameter B depends on the reflectivity of the seabed and the number of reflections of the sound, which depends on the grazing angle between the Mach cone and seabed. The DCS model presumes constant water depth and bottom properties, which were not present in the project area. Therefore, the linear model [Eq. (2)] used here fixes A at ten, uses a linear dependence on range (R), a sinusoidal dependence on the $\theta_{\mathrm{Pile\text{-}Rec}}$ and allows for a cross-term (E) between R and $\theta_{\mathrm{Pile\text{-}Rec}}$,

$$\mathrm{RL} = \mathrm{RL}_0 + A\mathrm{SE} + B\mathrm{PP} + CR + D\cos(\theta_{\mathrm{Pile-Rec}}) + E(R, \cos(\theta_{\mathrm{Pile-Rec}})) - (10\log_{10}R + \alpha(f)R). \quad (2)$$

The model includes terms for the SE, PP into the sediment, and a term to account for sound absorption by seawater, $\alpha(f)R$. The predictor variables are described further in Table II. The $10\log_{10}(R)$ and $\alpha(f)R$ terms are fixed effects that were accounted for by adding their values to the measured received levels before performing the linear regressions. Both the linear SE and PP, as well as logarithms of those values, were evaluated as covariates. The response variable in Eq. (2), RL, could be any per-strike acoustic metric.

Equation (2) is missing terms that account for variability in the propagation conditions such as different sound speed profiles, pile-receiver bathymetry, bottom composition, sea state, as well as changes in water depth due to tides. Using an advanced numerical propagation model as the basis for Eq. (2) rather than DCS from Lippert *et al.* (2018) would account for these factors as was previously performed by Wilkes and Gavrilov (2017). However, such a model is much more difficult to use for regressions with measured data and less intuitive for understanding the regression results. Instead, these factors may be investigated by using the random effects term of a linear mixed model. Random effects models group the measured observations based on data parameters and estimate an intercept offset coefficient for that group, so that the remaining linear coefficients better represent their underlying variability in the data. If the propagation effects are unimportant then a linear mixed model will not substantially improve the model goodness-of-fit compared to a standard linear model. Goodness-of-fit can be evaluated with the Akaike information criteria (AIC) and plots of residuals versus predictors (among many other

TABLE II. Predictor variables for the pile driving linear mixed models.

Parameter	Meaning
RL	**Received level**: any of the measured sound metrics ($L_{p,\mathrm{pk}}$, $L_{p,\mathrm{rms,0.125s}}$, $L_{E,0.125\mathrm{s}}$, and five $L_{E,0.125\mathrm{s},W}$ for the marine mammal auditory function weighted SEL (Southall *et al.*, 2019). Note that 24-hour SELs were computed by summing the per-strike values or modeling sound levels assuming 8000 strikes per day.
Constant	This is the intercept from the linear model in the same units as RL.
R	**Range**: from the pile in meters
SE	**Strike**: energy from pile driving logs in kilojoules
PP	**Pile penetration**: depth in meters that the pile has penetrated the seabed—range 0–60 m.
$\theta_{\text{Pile-Rec}}$	**Pile-recorder angle**: Angle between the recorder and pile, rotated so that if the Mach cone was headed directly at the recorder, the angle was 0. For pile-recorder geometries where the Mach cone was directed downward at the seabed, the value was 180 deg.
$\alpha(f)$	**Absorption:** seawater absorption term (e.g., François and Garrison, 1982). Fixed values were used for each metric: 0 dB/km for $L_{p,0.125\mathrm{s}}$, $L_{p,\mathrm{pk}}$, $L_{E,0.125\mathrm{s}}$, and $L_{E,0.125\mathrm{s,LF}}$; 0.25 dB/km for $L_{E,0.125\mathrm{s,OTA}}$ and $L_{E,0.125\mathrm{s,PHO}}$; 1 dB/km for $L_{E,0.125\mathrm{s,HF}}$ and $L_{E,0.125\mathrm{s,VHF}}$. These values of absorption were chosen as representatives of the frequencies with the most energy from the source in the passband of the auditory weighting functions. This term was included in the model to separate the known sea water absorption effects from the unknown range dependent effects.

methods). By comparing the goodness-of-fit with different random effects predictor variables the type of propagation dependence was determined. The random effects evaluated were: (1) date only (8 cases), which would indicate that sound speed profile was the most important effect; (2) the recording location (4 cases) which would indicate coarse bathymetry was an important effect; (3) foundation-recorder path (12 cases), which would indicate that the bathymetry and bottom composition were the most important effect; (4) the pile identification (ID; 24 cases), which would indicate that a time specific effect was most important (such as surface scattering); and (5) the date plus foundation-recorder path (28 cases), which would indicate all effects are important. Linear modeling was performed in the ***R*** programming language using the packages "nlme" for linear mixed modeling (Pinheiro *et al.*, 2017), "MASS" for standard linear modeling (Venables and Ripley, 2002) and "robustlmm" for robust linear mixed modeling (Koller, 2016). Robust mixed effects modeling was used to determine if outliers or heterogeneity affected the model results.

Data from all recorders were used in the linear regressions for peak SPL, SPL, low-frequency-cetacean, otariid, and phocid auditory frequency weighted SEL. Only data from the recorders at ranges shorter than 5000 m were used for the mid- and high-frequency cetacean auditory frequency weighted SEL because the signal-to-noise ratio at the longer range was too low.

D. Determining isopleth prediction intervals

Because the estimated isopleths are the result of a statistical fit, it is important to determine the prediction interval of the models and hence the maximum predicted isopleth distances. For linear mixed models, the recommended method of estimating prediction intervals is bootstrapping the model, which means running the model with a subset of the available data multiple times to test the range of predicted values. For each bootstrap run, 24 piles were selected randomly from the list with replacement (i.e., the same pile could be selected more than once). For each pile, a 1:20 decimated strike data set was used, where the starting sample for the decimation was randomly selected between 1 and 20. Each of the bootstrap models then predict the received sound level for three strike energies and PPs (2.5th, 50th, and 97.5th exceedance levels of all strikes measured), range (25 m step size), and $\theta_{\text{Pile-Rec}}$ (2 deg step size). This data array was searched to find the median isopleth ranges as well as the 2.5% and 97.5% prediction intervals. To be conservative, the predictions were made using the overall population fixed effects, and ignored the random effects since future measurements could be made along any radial and day. One thousand bootstrap runs were performed for each acoustic metric. For the daily SEL metrics, 8000 strikes were assumed to occur since the day with the highest number of strikes was Sept. 19 with 7812. For the daily SEL radii estimation we assumed that all strikes had the same per-strike SEL for three cases—the 2.5th, 50th (median), and 97.5th percentiles from the bootstrapped model.

The bootstrapping method of estimating prediction intervals for linear mixed models is computationally intensive for large data sets and requires a moderate computer programming capability. A faster and simpler method is desirable, especially for sound source characterizations that must report results within 24 h of data collection. Therefore, a second method was evaluated. A single linear mixed model run was generated using all the data, and the difference between the measured and modeled data was computed, using only the population fixed effects (again ignoring the random effects to be conservative). The predicted sound levels were then increased by the 97.5th percentile of the differences (i.e., the residuals), and the range to the isopleths computed using the offset predictions. This method is referred to as the "increase intercept" method since it effectively adds the offset to the intercept (constant) term of the linear models.

III. RESULTS

A. Measured sound levels

The measured sound levels generally decreased with range from the piles, but also depended on the pile-recorder angle (Fig. 2). For each pile the sound levels were approximately normally distributed about their mean values; however, the mean values changed with angle, which resulted in multiple protuberances in the sound level violin plots (Fig. 2, top) and

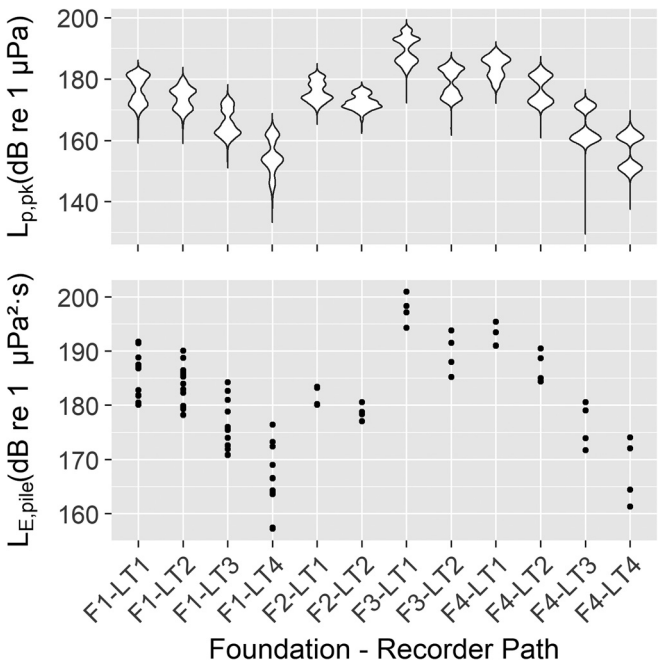

FIG. 2. Distribution of received sound levels by foundation-recorder path (see Fig. 1) for all detected impact pile driving impulses (range not to scale). (Top) Violin plots of peak SPLs. The different protuberances in each of the distributions correspond to different $\theta_{\text{Pile-Rec}}$ affecting the received sound levels. (Bottom) The per-pile SEL; each dot corresponds to a pile leg measurement made for the foundation-Recorder combination shown on the x axis. For foundation F1 all three pile sections were measured (three pile driving events).

up to 15 dB differences in the pile SEL for the same foundation - recorder geometry (Fig. 2, bottom). For example, consider the data for foundation 4 measured at recorder LT3 (F4-LT3, range was 4620 m) where all four foundation legs were measured. The 7856 detected impulses had two clusters of per-strike peak SPLs (Fig. 2, top). The measured per-pile SELs for the four legs were 172–182 dB re 1 μPa^2 s (Fig. 2, bottom). The pile-recorder angles, as well as variations in propagation conditions, hammer energy, PP into the sediment, and the total number of strikes per pile also influenced these sound levels. Detailed measurements from recorder LT1 for piling at foundation 3, section 2, leg B2 are shown in Fig. 3 (541 m range—the closest range measured). The sound levels rose in steps because of changes in SE and rose steadily throughout the pile driving as the pile penetrated deeper into the sediment [Figs. 3(A) and 3(B)]. The total pile SEL (L_E) increased rapidly during the first 200–300 strikes, but then increased more slowly throughout the remainder of the pile driving [Fig. 3(B)]. The energy was concentrated in the 100–800 Hz band [Fig. 3(C)].

B. Linear model of the measured sound levels

The linear and robust mixed models were both superior to the simple linear model in accounting for the dependencies in the data. The linear and robust linear mixed models had similar residual structures, prediction parameters, and hence similar performance. The linear mixed modeling approach was selected for further analysis using the bootstrapping analysis of the prediction intervals because each pass of the model was much faster than the robust version (hours versus days).

A wide variety of model definitions were evaluated before selecting the final form. Table III shows the model definition and AIC for various combinations of the predictor variables and random effects. A decrease in AIC of two is equivalent to a 1/e improvement in the likelihood of the model, so that a lower AIC is a better fit to the data. The model has three "spatial" terms—range, the cosine of the pile-recorder angle, and their cross-term. The AIC results indicate that removing the angle term results in a poorer representation of the measurements than removing the range term and including the cross-term results in the best agreement. The angle term indicates there is a variation in the attenuation that depends on the angle between the pile and recorder (0° means the pile is inclined away from the recorder and 180° means the pile is inclined toward the recorder—the sound is directed toward the seabed at a higher angle). The range term indicates that there is an attenuation of the sound that changes linearly with range so that the loss is greater than the fixed value of $10\log_{10}(R)$. The cross-term indicates that the range attenuation also changes with angle with greater attenuation when the pile is inclined toward the recorder at longer ranges. The model that is linear in SE and linear in PP had a much lower AIC than any of the models where these predictors were omitted or where the model included the logarithms of those variables.

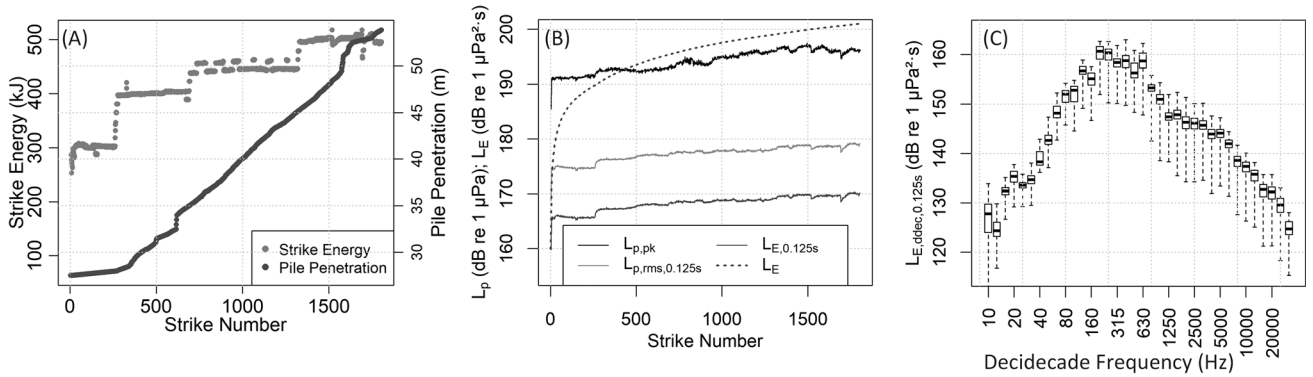

FIG. 3. Sound levels measured 541 m from the pile during installation of foundation 3, pile section 2, leg B2 (F3P2B2): (A) SE and PP; (B) time series of $L_{p,pk}$, $L_{p,\text{rms},0.125s}$, $L_{E,0.125s}$, as well as the accumulation of the total pile L_E. (C) Distribution of $L_{E,0.125s,\text{ddec}}$.The mean background decidecade SEL (0.125 s integration time) was below 120 dB re 1 μPa^2 s for all bands and is not shown.

TABLE III. AIC for different linear mixed model definitions and random effects for the low-frequency cetacean auditory frequency weighted per-strike SELs (Southall *et al.*, 2019). The covariate abbreviations are: *R*, range; SE, strike energy; PP, pile penetration; $\vartheta_{\text{Pile-Rec}}$ is the pile-recorder angle; $X_{R\vartheta}$ is the range-angle cross-term. *A*, *B*, *C*, *D*, and *E* are the model fit parameters. The intercept term and $10\log_{10}(R)$ are assumed and not explicitly included. "Fdn" is the Foundation number (F1–F4) and "Rec" is the recorder ID (LT1–LT4).

Model definition	Random effect (number of unique effects)	AIC
LF SEL $\sim A\text{SE} + B\text{PP} + CR + D\cos(\vartheta_{\text{Pile-Rec}}) + EX_{R\vartheta}$	Date-Fdn-Rec (28)	400374
LF SEL $\sim A\text{SE} + B\log_{10}(\text{PP}) + CR + D\cos(\vartheta_{\text{Pile-Rec}}) + EX_{R\vartheta}$	Date-Fdn-Rec (28)	402462
LF SEL $\sim A\text{SE} + CR + D\cos(\vartheta_{\text{Pile-Rec}}) + EX_{R\vartheta}$	Date-Fdn-Rec (28)	403243
LF SEL $\sim A\log_{10}(\text{SE}) + B\text{PP} + CR + D\cos(\vartheta_{\text{Pile-Rec}}) + EX_{R\vartheta}$	Date-Fdn-Rec (28)	407209
LF SEL $\sim A\log_{10}(\text{SE}) + B\log_{10}(PP) + CR + D\cos(\vartheta_{\text{Pile-Rec}}) + EX_{R\vartheta}$	Date-Fdn-Rec (28)	411042
LF SEL $\sim A\text{SE} + B\text{PP} + CR + D\cos(\vartheta_{\text{Pile-Rec}}) + EX_{R\vartheta}$	Fdn-Rec (12)	417085
LF SEL $\sim B\text{PP} + CR + D\cos(\vartheta_{\text{Pile-Rec}}) + EX_{R\vartheta}$	Date-Fdn-Rec (28)	419515
LF SEL $\sim A\text{SE} + B\text{PP} + CR + D\cos(\vartheta_{\text{Pile-Rec}})$	Date-Fdn-Rec (28)	420186
LF SEL $\sim A\text{SE} + B\text{PP} + D\cos(\vartheta_{\text{Pile-Rec}})$	Date-Fdn-Rec (28)	420234
LF SEL $\sim A\text{SE} + B\text{PP} + CR + D\cos(\vartheta_{\text{Pile-Rec}}) + EX_{R\vartheta}$	Date (4)	459114
LF SEL $\sim A\text{SE} + B\text{PP} + CR$	Date-Fdn-Rec (28)	555720

The date-foundation-recorder random effect greatly reduced the AIC and was selected as the best model. This random effect represents each combination of date and pile-to-recorder path as a unique structure. The random effects are adjustments to the model's intercept term. Ninety-nine percent of the random effects' coefficients had a magnitude of less than 6 dB, and 83% of them were below 3 dB. The distribution of the random effects as a function of acoustic metric response variable, date, and pile-recorder radial are shown in Fig. 4. The linear mixed model coefficients and standard deviations determine by the bootstrapping analysis are shown in Table IV. The PP and SE coefficients estimated with a simple linear model (rather than the linear mixed model) were within 10% of the values found for the linear mixed model but with higher standard deviations, indicating that these covariates are an important and repeatable part of the model.

The interactions of the model terms are difficult to visualize from Table IV. Figure 5 provides predictions of the low-frequency cetacean auditory frequency weighted SEL for bearings of 0–360 deg and for the 12 pile-recorder paths measured during the long-term program. The predictions are overlaid with the per-strike $L_{E,0.125\text{s,LF}}$ from all measurements. The range–angle interaction increases the attenuation with range when the pile was inclined toward the recorder (180 deg) compared to orientations where the piles were inclined away from the recorders (0 and 360 deg). The median hammer SE and PPs were used for the median predictions in Fig. 5, while the 2.5th and 97.5th percentiles of the strike energies and PPs were used for the dashed prediction intervals in Fig. 5.

IV. DISCUSSION

This analysis of the Block Island Wind Farm long-term data using a linear mixed model identified two types of variabilities that affected the received sound levels measured 540–9100 m from the impact pile driving: (1) variability in the source factor, i.e., the emitted sound levels depended on the SE and PP; and (2) variability in the propagation conditions, which included the inclination of the pile, source-receiver path effects, and date/time related effects. The results are informative for the development of pile driving acoustic propagation models, and determining how to establish sound level isopleths for the monitoring of marine life during future offshore pile driving to install wind turbines. The results are also useful for extending the range of validity of the empirical peak SPL versus SEL relationship proposed by Lippert *et al.* (2015).

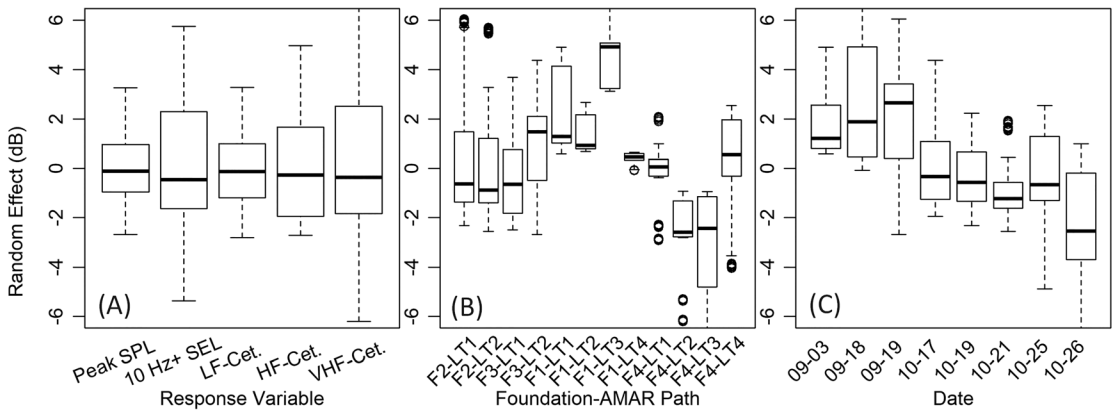

FIG. 4. Distribution of the random effect intercept coefficients. The data were obtained by running the model for five response variables (peak SPL, 10 Hz and above SEL, and the LF-, HF-, and VHF-cetacean auditory frequency weighted SEL). For each response variable the model was evaluated ten times with a random selection of 1/10th of the complete data set.

TABLE IV. Mean (standard deviation) coefficients for the DCS-based linear mixed model [A, B, C, D, and E in Eq. (2)]. The standard deviations were obtained using 1000 bootstrapping model runs where each run used 5% of the dataset. LF, HF, VHF, OTA, and PHO are the Southall *et al.* (2019) low-, high-, and veryhigh-frequency cetacean as well as otariid and phocid pinniped marine mammal hearing group auditory weighting functions. Eight thousand strikes were used for computing the daily SELs.

Sound metric	Intercept (dB)	ASE (dB/kJ)	BPP (dB/m)	CR (dB/km)	D cos($\theta_{\text{Pile-Rec}}$) (dB)	$EX_{R\theta}$ (dB/km)
$L_{p,\text{pk}}$	207 (0.90)	0.0115 (0.004)	0.0550 (0.021)	−2.12 (0.12)	4.66 (0.50)	0.15 (0.10)
$L_{p,\text{rms}}$	194 (0.74)	0.0116 (0.003)	0.0292 (0.016)	−1.74 (0.10)	2.87 (0.45)	0.4 (0.10)
$L_{E,0.125\text{s}}$	185 (0.74)	0.0116 (0.003)	0.0291 (0.016)	−1.75 (0.10)	2.89 (0.43)	0.4 (0.10)
$L_{E,0.125\text{s,LF}}$	183 (0.78)	0.0114 (0.003)	0.0451 (0.018)	−1.86 (0.09)	2.89 (0.49)	0.4 (0.10)
$L_{E,0.125\text{s,OTA}}$	173 (0.76)	0.0105 (0.003)	0.0867 (0.018)	−2.08 (0.12)	3.28 (0.60)	0.17 (0.14)
$L_{E,0.125\text{s,PHO}}$	173 (0.74)	0.0106 (0.003)	0.0777 (0.018)	−1.95 (0.11)	3.12 (0.55)	0.25 (0.12)
$L_{E,0.125\text{s,HF}}$	159 (0.97)	0.0096 (0.003)	0.0742 (0.022)	−1.72 (0.17)	2.61 (0.56)	0.006 (0.09)
$L_{E,0.125\text{s,VHF}}$	154 (1.07)	0.0094 (0.003)	0.0704 (0.023)	−1.79 (0.18)	2.38 (0.53)	0.022 (0.09)

A. Variability in sound levels

The long-term data from monitoring of the Block Island Wind Farm provided enough data to evaluate a novel method of analyzing pile driving sound levels: the use of a linear mixed model based on DCS (Lippert *et al.*, 2018). The random effect in the linear mixed model was designed as an offset to the linear model's intercept term based on date and pile-to-recorder path. Thus, the model provides information about the acoustic propagation variability and dependence of the source factor on SE and PP.

The coefficients for SE varied by sound metric (Table IV). The coefficient for SE was slightly smaller for metrics where the data have more high-frequency dependence (e.g., the pinniped and odontocete weighted SEL). The SE term

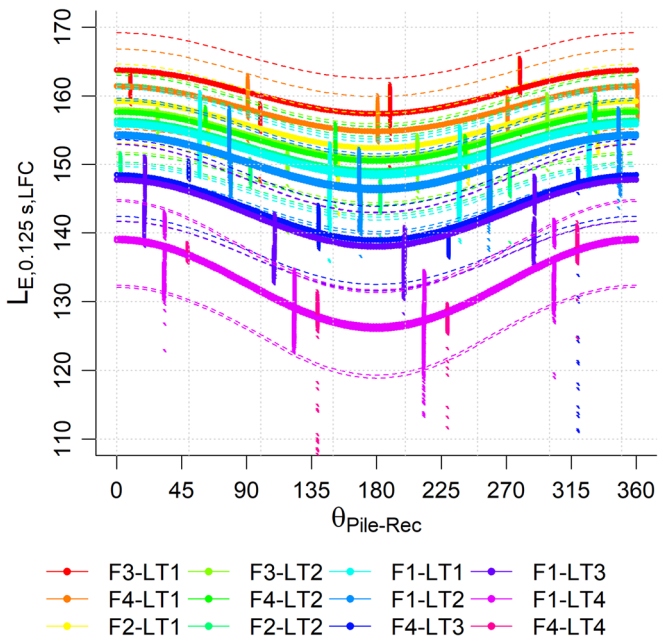

FIG. 5. (Color online) Measured (dots) and modeled (lines) $L_{E,0.125\text{s,LF}}$ (dB re 1 μPa^2 s) versus the pile-recorder angle ($\vartheta_{\text{Pile-Rec}}$) for all data collected during the long-term monitoring program at Block Island. Solid lines show the median predicted $L_{E,0.125\text{s,LF}}$ (from the 1000 bootstrapping model runs) for the 12 pile-recorder paths using the median hammer SE and PPs and the coefficients in Table IV. The dashed lines are the 95% prediction interval (2.5th–97.5th percentiles of 1000 bootstrapping runs). The complete set of all measured $L_{E,0.125\text{s,LF}}$ are overlaid, adjusted by the per-pile random effects coefficients.

serves to increase the model intercept term [Eq. (2)] by 0.0094–0.0116 dB/kJ. The mixture of linear and logarithmic units was unexpected, but this combination was strongly preferred by that AIC and was therefore selected as the best model (Table III; this is also how the modeling was performed in Bailey *et al.*, 2010). Since the minimum and maximum SEs were 74 kJ and 684 kJ, the predicted sound levels increased up to 7.9 dB because of changes in the SE, which will substantially increase the biological effects isopleths. For comparison, Robinson *et al.* (2007) measured the ramp up of pile driving energy from 80 to 800 kJ over 800 strikes and found an increase in broadband SEL of 8 dB and the peak-to-peak SPL increased 10–12 dB (i.e., the maximum peak SPL to compressional peak SPL). The model coefficients found here are very similar: a 7.9 dB increase in SEL and peak SPL (nominally a 13.9 dB increase in peak-to-peak SPL) for the range of strike energies measured by Robinson *et al.* (2007). The Robinson *et al.* (2007) results did not separate possible effects of PP from the SE increases.

The model indicated that sound levels rose as the pile penetrated the sediment for all metrics. The PP coefficient was higher for the metrics that depend on high-frequency content, including $L_{p,\text{pk}}$, and the otariid, phocid, high-, and very high-frequency cetacean auditory frequency weighted SEL (Table IV). The maximum penetration of the piles at the Block Island Wind Farm was 60 m, so the effective increase in the model's intercept term (i.e., the initial sound level at 0 m, which is *not* the source level), ranged from ∼1.8 dB for $L_{p,\text{rms}}$ and $L_{E,24\text{h}}$; ∼2.7 dB for $L_{E,24\text{h,LF}}$, and 4–5 dB for $L_{E,24\text{h,HF}}$, $L_{E,24\text{h,VHF}}$, $L_{E,24\text{h,OTA}}$, and $L_{E,24\text{h,PHO}}$. MacGillivray (2014) reported that measured sound levels at frequencies above 600 Hz were higher than predicted by a pile sound source model that agreed very well with measurements below 600 Hz. The possible sources of mismatch were identified as an incorrect spectrum in the source forcing function, or excitation of higher order vibration modes in the pile. The increase in sound levels at higher frequencies with penetration found here supports the idea that higher order vibrations are being excited in the piles, since both the free length of the pile and how tightly the pile toe is held will affect the frequency and amplitude of those vibrations. The PP results are useful for several purposes. First, the higher auditory frequency weighted SEL have significant energy contributions starting at ∼2 kHz (Southall *et al.*, 2019),

which is higher than the 2–3 kHz that is the top frequency for most pile driving source models (Lippert *et al.*, 2016). The current results should inform the development of improved high-frequency modeling capabilities so that accurate estimates of the possible effects of pile driving on pinnipeds and odontocetes may be performed. Note that those are the marine mammal species groups most likely to be found in the shallow waters where pile driving occurs. Second, the variation in sound levels with PP changes the isopleths during the pile driving, even if the SE remains unchanged. Variable isopleths are discussed in Sec. IV B.

The range and directional variability in received levels was modeled in Eq. (2) by the fixed $10\log_{10}(R) + \alpha(f)\cdot R$, a range term ($CR$), the cosine of the pile-recorder angle [$D\cos(\vartheta_{\text{Pile-Rec}})$], and the range-direction cross-term. The largest source of variability in the sound levels measured at Block Island was the inclination angle between the pile and the seabed in the direction of the receiver. This was also noted during finite element modeling and measurement of raked (inclined) piles by Wilkes and Gavrilov (2017). When the pile is inclined toward the receiver there are more interactions with the surface and seabed, which attenuates the received sound levels. The coefficient of the angle term in the model was 2.38–3.28 dB, except for the peak SPL whose coefficient was 4.66 (Table IV). This term multiplies by the cosine of the pile-recorder angle, which has a value of one when the pile is inclined away from the recorder and −1 when inclined toward the recorder. The angle term was amplified by the range-angle cross-term, for example, a value of 0.4 dB/km for the low-frequency cetacean auditory frequency weighted SEL. Thus at 5 km from the pile, the model predicts the sound levels inclined toward the pile were 10 dB higher than those when inclined away from the pile, which are approximately the ranges for the LT3 measurements in Fig. 5. The implication of these results, Wilkes and Gavrilov (2017), and an inclined version of DCS (Lippert *et al.*, 2018) is that modeling and measurements of inclined piles for regulatory compliance must consider the orientation of the piles and its effects on the biological isopleths.

The random effects corrections of the linear mixed model represented useful information about the function of the model and the acoustic propagation conditions. The random effects did not depend on the response variable [Fig. 4(A)] as expected for correct functioning of the model. The boxplots of random effects coefficients versus pile-to-recorder path are roughly grouped into three blocks—propagation from foundations F2 and F3, then F1, and finally F4 [Fig. 4(B)], meaning there are different propagation effects along these paths that do not depend on time and are likely due to small-scale bathymetry and sediment composition differences. These types of variations due to small changes in propagation conditions were predicted by the Monte Carlo simulations of Lippert and Estorff (2014). The random effects corrections plotted against date show two clusters—the first three in September have mean corrections above zero, and the five in October have corrections below zero [Fig. 4(C)]. This view of the random effects appears to have detected changes in the sound speed profile, which was upward refracting in September and iso-velocity in October.

B. Effects of sound level variability on isopleths

The linear mixed model was developed to understand the variability in the measured sound levels, which provided insights into changes in the initial sound level (the constant or intercept term in the model) as well as propagation conditions. Often linear models of sound levels from human activities with range are created to estimate the biological effects of isopleth distances. This study estimated the median isopleths, as well as the prediction interval, of the models. The median isopleths were lower than the pre-construction estimates for all biological effects' thresholds and propagation directions (the 206 dB re 1 μPa $L_{p,\text{pk}}$ and 207 dB re 1 μPa $L_{p,0.125\text{s}}$ could not be extrapolated from the measurements without extending the regressions too far from the minimum measurement distance of 541 m). For the case of sea turtle behavioral disturbance, ranges longer than permitted were predicted by the model when the strike energies where high and the piles were near refusal (i.e., at full penetration depth; see Tables I and V).

The sources of variability result in isopleth distances that are neither symmetric nor constant (e.g., Fig. 6). They depend on SE and PP that change over the duration of the piling and on random fluctuations in the piling and propagation conditions. The effects on regulatory radii are more exaggerated for isopleths that have longer ranges with fewer seabed and surface interactions (e.g., Fig. 6 and Table V). The effect of the SE and PP on the isopleth distances are fixed effects that are predictable; however, their effects are compounded by the directional effect. Figure 6 demonstrates this using the prediction interval from the model—the distance doubled for a pile inclined toward the recorder but went up by almost a factor of four for a pile inclined away from the recorder. The effect is further demonstrated in Fig. 7 and shows the sea turtle disturbance isopleth of 166 dB re 1 μPa $L_{p,\text{rms}}$ as it evolved over one piling event—pile F3P2B2 on 18 Sept 2015 (also shown in Fig. 3). During this piling event the SE increased from 308 kJ to 518 kJ, and the PP increased from 28 m to 54 m. The isopleth distances increased by ∼70% when the pile was inclined away from the recorder but only increased by ∼40% when the pile was inclined toward the recorder. These results show the importance of including accurate treatment of the SE and PP in acoustic propagation modeling of pile driving. Cushioning materials between the hammer and pile head are also a key component of accurate modeling of how SE converts to radiated energy (MacGillivray, 2014).

The variability measured here results in longer biological effects isopleths as pile-driving progresses. A quick but accurate method of determining the maximum distance is desired. The bootstrapping and increased intercept methods of estimating the maximum isopleth distance are compared in Table VI. Both methods produced the same median isopleth distance for all three cases and all three metrics. The maximum isopleth distances differed by at most 2% between methods. The increased intercept method is recommended for most applications due to ease of computation.

C. Relationship between peak sound pressure level and sound exposure level

Lippert *et al.* (2015) discussed the difficulties in modeling the peak (and peak-to-peak) SPL due to scattering from

TABLE V. Example isopleths (m) using the Block Island Wind Farm data and the linear mixed model for selected biological effects thresholds from NMFS and NOAA (1995); Popper *et al.* (2014), and Southall *et al.* (2019). Ranges are shown for three conditions: (1) the loudest case—the pile inclined away from the recorder with 97.5th percentile of the hammer energy (644 kJ) and penetration depth (56 m); (2) the median case of a vertical pile and the median hammer SE (392 kJ) and PP (38 m); and (3) the quietest case—the pile inclined toward the recorder with 2.5th percentile of the hammer SE (74 kJ) and PP (8 m). The bold number at the center of each box is the median range. The lower-left and upper-right numbers are the lower and upper prediction intervals (2.5th and 97.5th percentiles, respectively), obtained by bootstrapping the linear mixed effects model 1000 times for each of the acoustic metrics and predicting the sound levels at range steps of 25 m. PTS is the threshold for permanent hearing threshold shift.

Isopleth metric	Regulatory threshold	Longest-distances: Pile inclined away from recorder with 644 kJ hammer energy and 56 m PP	Median distances: Vertical pile with 392 kJ hammer energy and 38 m PP	Shortest distances: Pile inclined toward recorder with 74 kJ hammer energy and 8 m PP
Fish unweighted recoverable injury[a]	203 dB re 1 μPa^2 s $L_{E,24h}$	1725 **750** <250[b]	1000 **425** <250[b]	550 **<250**[b] <250[b]
LF weighted PTS[c]	183 dB re 1 μPa^2 s $L_{E,24h,LF}$	9450 **6625** 4025	6450 **4600** 2625	4600 **3150** 1600
Turtle disturbance[d]	166 dB re 1 μPa $L_{p,0.125s}$	4025 **2300** 925	2600 **1425** 525	1650 **825** 250
Marine mammal level B take[e]	160 dB re 1 μPa $L_{p,0.125s}$	6850 **4575** 2400	4575 **3000** 1450	3125 **1925** 800
VHF weighted PTS[c]	155 dB re 1 μPa^2 s $L_{E,24h,VHF}$	5375 **4500** 2875	4700 **3400** 1925	4100 **2850** 1375

[a]Popper *et al.* (2014), Table VII.3.
[b]Because the shortest measurement range was 541 m, it was not appropriate to extrapolate the regressions closer to the pile than 250 m.
[c]Southall *et al.* (2019).
[d]BIWF Biological Opinion.
[e]NMFS and NOAA, 1995.

the rough seabed and surface. The SEL, however, is relatively straightforward to model and numerous accurate methods exist (for frequencies below 2 kHz; Lippert *et al.*, 2016). In Lippert *et al.* (2015) they demonstrate that there is a linear relationship between the peak-to-peak SPL and the SEL using data from three North Sea piling operations in water depths of 27–40 m. The linear relation is given as

$$L_{p,\mathrm{pk}} = AL_{E,0.125\mathrm{s}} + B. \quad (3)$$

It is desirable to know if the relationship holds for the Block Island data. The coefficient values obtained by Lippert *et al.* (2015) were $A \sim 1.4$ and $B \sim -40$ dB. In the present study $L_{p,\mathrm{pk}}$ was used instead of $L_{p,\mathrm{pk\text{-}pk}}$ since the regulatory threshold for fish used the $L_{p,\mathrm{pk}}$ metric (Table I). When the L_E was restricted to the same range of values as measured by Lippert *et al.* (2015) (155–170 dB re 1 μPa^2 s) the model coefficients from Eq. (3) were $A = 1.36$ and $B = -34$ [Fig. 8(A)]. This is in excellent agreement with the previous results, noting that $L_{p,\mathrm{pk\text{-}pk}}$ will be approximately 6 dB greater than $L_{p,\mathrm{pk}}$ and hence the intercept term B reported here should also be ~6 dB greater (Lippert *et al.*, 2015, reported differences of 5.3–5.7 dB between peak and peak-to-peak SPLs). Due to the effects of pile inclination, the 95% confidence interval on the peak SPL for the Block Island data was 3.2 dB, more than double the 1–1.5 dB reported by Lippert *et al.* (2015). For the full range of per-strike L_E measured at the Block Island Wind Farm, a two-segment line fit provided a better fit than a single linear model [Fig. 8(B)]. For SEL above 154 dB the same equation was obtained. For SEL below 154 dB the parameters were $A = 1.06$ and $B = 11$. Thus, a slightly modified version of the Lippert *et al.* (2015) relationship holds over a broad range of

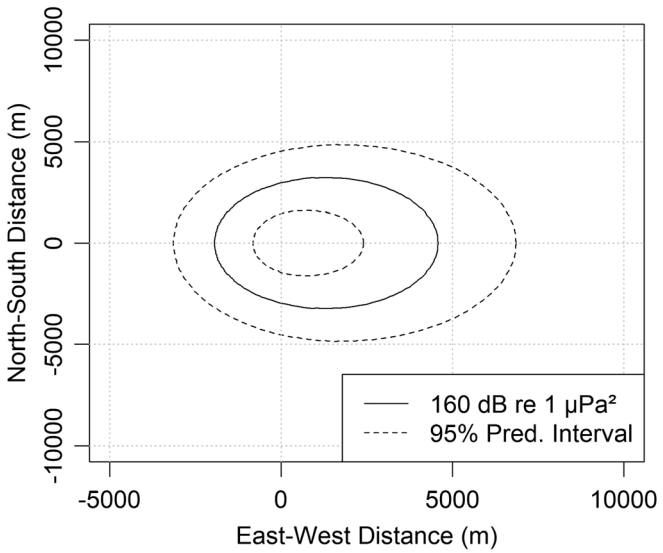

FIG. 6. Bootstrapped predictions of the Block Island Wind Farm radii of biological effects for the 160 dB re 1 μPa^2 s $L_{p,0.125s}$ isopleth (see Table I) with 2.5 and 97.5% prediction intervals. The isopleths are non-circular because of the directional sound propagation effects with the inclined piles. Zero degrees in Fig. 5 is to the right in this figure.

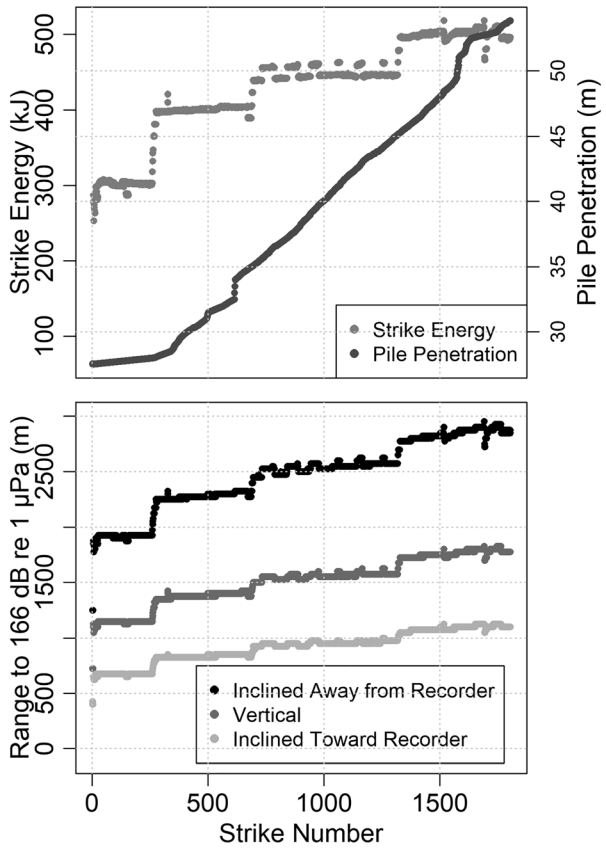

FIG. 7. Estimate of the range to the sea turtle disturbance SPL (166 dB re 1 μPa) using the actual strike energies and PPs from pile F3P2B2 on 18 Sept 2015. (Top) Time history of the SE and PP, same data as Fig. 3(A). (Bottom) The modeled ranges to a per-strike SPL of 166 dB re 1 μPa.

SEL and peak SPL; however, the confidence intervals are wider due to the effects of pile inclination.

D. Recommendations for recording and analyzing pile driving biological effects radii

Accurate measurement of the distances to possible biological effects from anthropogenic activity requires careful attention to detail. For data collection:

(1) Perform numerical acoustic modeling beforehand to estimate the radii. Assume at least a ± 3 dB variability in source factor to estimate the possible range of radii.
(2) Place one recorder at or near the shortest expected isopleth distance, and another at or beyond the furthest isopleth distance you wish to estimate. Confidence intervals are much larger outside the range span measured.
(3) Use at least three recorders, however, four are highly recommended when the range span of interest is larger than 1–2 km.
(4) Logarithmically space recorders in range in as straight a line from the pile as possible.
(5) Place all recorders at the same depth where possible; being in a straight line is more important.
(6) For water depths less than 50 m, a single hydrophone on the bottom will suffice in most conditions. For deeper waters with complex propagation conditions, a second hydrophone in the water column may be needed—the acoustic propagation modeling will help inform this choice.
(7) For inclined piles, monitor along the radial with the pile inclined away from the recorders.

With respect to data analysis:

(1) Process all events with a fixed window duration; 0.125 s is recommended.
(2) Use a systematic, repeatable method to remove outliers and false alarms from the data.
(3) For single radial measurements, fit the data to an equation of the form $\mathrm{RL} = \text{constant} - 10\log_{10}R + BR$, where B should be negative (Lippert *et al.*, 2018).
(4) For multiple pile or radial measurements use a linear mixed model, where the random effect is the date-recorder-pile combination.
(5) Estimate and include the prediction intervals by determining an offset for the model's constant term that results in 97.5% of the measured data being less than the model fit.
(6) During detailed post analysis include the hammer SE and PP data as co-variates if they are available.

For analysis of a single piling event, the linear models will produce the same result whether their input is a single mean value for the acoustic metrics or the value for each individual impulse. In these cases, computing the one-minute peak SPL and SELs is simpler and will generate equivalent results. The one-minute method should not be used for SPL metrics.

TABLE VI. Comparing methods of determining the isopleth distance prediction interval. Method 1: 1000 bootstrapped model runs, method 2: perform a single linear mixed model run, then increase the intercept term so that 97.5% of the measured data points are below the prediction line. Bold values in the bottom left of each cell are the median isopleths. The value in the top right-hand corner of each cell is the 97.5th percentile prediction interval maximum.

Isopleth metric	Regulatory threshold	Prediction interval modeling method	Longest-distances: Pile inclined away from recorder with 644 kJ hammer energy and 56 m PP		Median distances: Vertical pile with 392 kJ hammer energy and 38 m PP		Shortest distances: Pile inclined toward recorder with 74 kJ hammer energy and 8 m PP	
Turtle disturbance	166 dB re 1 μPa $L_{p,0.125s}$	Bootstrapping	4025	**2300**	2600	**1425**	1650	**825**
		Increase intercept	4050	**2300**	2625	**1425**	1650	**825**
Marine mammal level B take	160 dB re 1 μPa $L_{p,0.125s}$	Bootstrapping	6850	**4575**	4575	**3000**	3125	**1925**
		Increase intercept	6875	**4575**	4625	**3000**	3125	**1925**
Fish disturbance	150 dB re 1 μPa $L_{p,0.125s}$	Bootstrapping	13075	**9575**	8775	**6750**	6350	**4775**
		Increase intercept	13150	**9575**	8825	**6750**	64	**4775**

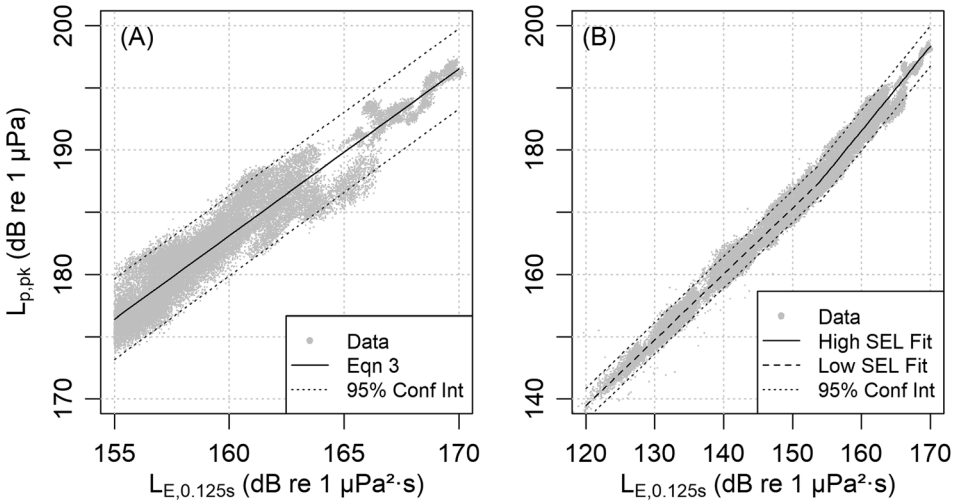

FIG. 8. Per-strike SEL ($L_{E,0.125s}$) versus peak SPL ($L_{p,pk}$) and regression curves. (A) Restricting the L_E to the range reported in Lippert *et al.* (2015). (B) The full $L_{E,0.125s}$ range measured at Block Island Wind Farm.

ACKNOWLEDGMENTS

The author would like to thank Deepwater Wind/Block Island Wind Farm for making this data set available for publication and JASCO Applied Sciences for support preparation of this manuscript. Thanks to JASCO's engineering and field teams for developing and deploying the moorings that successfully recorded this data set. The logistics and field work components were arranged and supported by Tetra Tech Inc. and performed from the fishing vessel (F/V) *Heather Lynn*. Thanks to Robert Mills, David Zeddies, and Jeff MacDonnell of JASCO for assistance with the original data analysis for Block Island Wind Farm that was the starting point for this analysis. Thanks to Joanna Mills-Flemming for assistance with setting up and understanding the operation of linear mixed models and robust linear mixed models. Sound speed profile data were supplied by Tetra Tech Inc. Thanks to Michael Ainslie for his reviews of early versions of the manuscript, in particular, for pointing out the newly published article (Lippert *et al.*, 2018) that became an integral part of this analysis. Thanks to the anonymous reviewers of the manuscript who challenged me to generalize the discussion and provide more insights into the PP and SE results.

[1]See https://bit.ly/2PyxSXB for harassment authorization and https://bit.ly/2PCn0rC for United States Army Corps of Engineers permit (Last viewed 25 February 2019).

[3]See supplementary material at https://doi.org/10.1121/1.5114797 for (1) details of the recorder configurations and locations; (2) details of the Teager-Kaiser impulse detector; (3) pile locations and the 24 pile driving events analyzed; (4) typical data from all recorders for a single pile; (5) measured sound speed profiles; (6) examples of the pile driving logs; (7) further details on the performance of the linear models; (8) isopleth radii for the Block Island Wind Farm pile driving using a wide selection of regulatory thresholds; and (9) the outline for "R"-code to perform the linear mixed modeling and prediction interval estimation.

[4]See www.python.org (Last viewed 25 February 2019).

[2]NOAA Formal ESA Section 7 Consultation for Deepwater Wind, 30 Jan 2014, Table IX, available at https://bit.ly/2Q7P5Gw (Last viewed 25 February 2019).

Ainslie, M. A., Dahl, P. H., De Jong, C. A. F., and Laws, R. M. (**2014**). "Practical spreading laws: The snakes and ladders of shallow water acoustics," in *UA2014-2nd International Conference and Exhibition on Underwater Acoustics* (Island of Rhodes, Greece), pp. 879-886.

ANSI (**2006**). ANSI S1.4-1983. *American National Standard Specification for Sound Level Meters* (American National Standards Institute, New York).

Bailey, H., Senior, B., Simmons, D., Rusin, J., Picken, G., and Thompson, P. M. (**2010**). "Assessing underwater noise levels during pile-driving at an offshore windfarm and its potential effects on marine mammals," Mar. Pollut. Bull. **60**, 888–897.

Betke, K. (**2008**). "Measurement of wind turbine construction noise at Horns Rev II," Technical report by Institut für technische und angewandte Physik GmbH (ITAP) for BioConsultSH, Husun, Germany, p. 30.

Brandt, M. J., Diederichs, A., Betke, K., and Nehls, G. (**2011**). "Responses of harbour porpoises to pile driving at the Horns Rev II offshore wind farm in the Danish North Sea," Mar. Ecol. Prog. Ser. **421**, 205–216.

Casper, B. M., Halvorsen, M. B., Carlson, T. J., and Popper, A. N. (**2017**). "Onset of barotrauma injuries related to number of pile driving strike exposures in hybrid striped bass," J. Acoust. Soc. Am. **141**, 4380–4387.

Casper, B. M., Smith, M. E., Halvorsen, M. B., Sun, H., Carlson, T. J., and Popper, A. N. (**2013**). "Effects of exposure to pile driving sounds on fish inner ear tissues," Comp. Biochem. Physiol. A Mol. Integr. Physiol. **166**, 352–360.

Dahl, P. H. (**2015**). "The underwater sound field from impact pile driving and its potential effects on marine life," Acoust. Today **11**, 7(2), 18–25, available at https://acousticstoday.org/the-underwater-sound-field-from-impact-pile-driving-and-its-potential-effects-on-marine-life-peter-h-dahl-christ-a-f-de-jong-and-arthur-n-popper.

Dahl, P. H., and Dall'Osto, D. R. (**2017**). "On the underwater sound field from impact pile driving: Arrival structure, precursor arrivals, and energy streamlines," J. Acoust. Soc. Am. **142**, 1141–1155.

Dähne, M., Gilles, A., Lucke, K., Peschko, V., Adler, S., Krügel, K., Sundermeyer, J., and Siebert, U. (**2013**). "Effects of pile-driving on harbour porpoises (*Phocoena phocoena*) at the first offshore wind farm in Germany," Environ. Res. Lett. **8**, 025002.

Erbe, C. (**2013**). "International regulation of underwater noise," Acoust. Aust. **41**, 12–19, available at http://hdl.handle.net/20.500.11937/30038.

Erbe, C., Reichmuth, C., Cunningham, K., Lucke, K., and Dooling, R. (**2016**). "Communication masking in marine mammals: A review and research strategy," Mar. Pollut. Bull. **103**, 15–38.

Finneran, J. J. (**2015**). "Noise-induced hearing loss in marine mammals: A review of temporary threshold shift studies from 1996 to 2015," J. Acoust. Soc. Am. **138**, 1702–1726.

Finneran, J. J., Schlundt, C. E., Dear, R., Carder, D. A., and Ridgway, S. H. (**2002**). "Temporary shift in masked hearing thresholds in odontocetes after exposure to single underwater impulses from a seismic watergun," J. Acoust. Soc. Am. **111**, 2929–2940.

Finneran, J. J., Trickey, J. S., Branstetter, B. K., Schlundt, C. E., and Jenkins, K. (**2011**). "Auditory effects of multiple underwater impulses on bottlenose dolphins (*Tursiops truncatus*)," J. Acoust. Soc. Am. **130**, 2561–2561.

Fisheries Hydroacoustic Working Group (FHWG) (**2008**). "Agreement in principle for interim criteria for injury to fish from pile driving activities," available at http://www.dot.ca.gov/hq/env/bio/files/fhwgcriteria_agree.pdf.

François, R. E., and Garrison, G. R. (**1982**). "Sound absorption based on ocean measurements: Part II: Boric acid contribution and equation for total absorption," J. Acoust. Soc. Am. **72**, 1879–1890.

Halvorsen, M. B., Casper, B. M., Woodley, C. M., Carlson, T. J., and Popper, A. N. (**2011**). "Hydroacoustic impacts on fish from pile installation," (National Cooperative Highway Research Program, Transportation Research Board, National Academy of Sciences, Washington, DC).

Halvorsen, M. B., Casper, B. M., Woodley, C. M., Carlson, T. J., and Popper, A. N. (**2012**). "Threshold for onset of injury in Chinook salmon from exposure to impulsive pile driving sounds," PLoS One **7**, e38968.

ISO (**2017**). 18405.2:2017, *Underwater acoustics—Terminology* (International Organization for Standardization, Geneva, Switzerland).

Kandia, V., and Stylianou, Y. (**2006**). "Detection of sperm whale clicks based on the Teager-Kaiser energy operator," Appl. Acoust. **67**, 1144–1163.

Kastelein, R. A., Helder-Hoek, L., Van de Voorde, S., von Benda-Beckmann, A. M., Lam, F.-P. A., Jansen, E., de Jong, C. A. F., and Ainslie, M. A. (**2017**). "Temporary hearing threshold shift in a harbor porpoise (*Phocoena phocoena*) after exposure to multiple airgun sounds," J. Acoust. Soc. Am. **142**, 2430–2442.

Koller, M. (**2016**). "robustlmm: An R package for robust estimation of linear mixed-effects models," J. Statist. Software **75**, 1–24.

Lippert, T., Ainslie, M. A., and von Estorff, O. (**2018**). "Pile driving acoustics made simple: Damped cylindrical spreading model," J. Acoust. Soc. Am. **143**, 310–317.

Lippert, T., Galindo-Romero, M., Gavrilov, A. N., and von Estorff, O. (**2015**). "Empirical estimation of peak pressure level from sound exposure level. Part II: Offshore impact pile driving noise," J. Acoust. Soc. Am. **138**, EL287–EL292.

Lippert, S., Nijhof, M., Lippert, T., Wilkes, D., Gavrilov, A., Heitmann, K., Ruhnau, M., von Estorff, O., Schäfke, A., Schäfer, I., Ehrlich, J., MacGillivray, A. O., Park, J., Seong, W., Ainslie, M. A., deJong, C., Wood, M. A., Wang, L., and Theobald, P. (**2016**). "COMPILE—A generic benchmark case for predictions of marine pile-driving noise," IEEE J. Ocean. Eng. **41**, 1061–1071.

Lippert, T., and von Estorff, O. (**2014**). "The significance of parameter uncertainties for the prediction of offshore pile driving noise," J. Acoust. Soc. Am. **136**, 2463–2471.

Lucke, K., Siebert, U., Lepper, P. A., and Blanchet, M.-A. (**2009**). "Temporary shift in masked hearing thresholds in a harbor porpoise (*Phocoena phocoena*) after exposure to seismic airgun stimuli," J. Acoust. Soc. Am. **125**, 4060–4070.

Lucke, K., Winter, E., Lam, F.-P., Scowcroft, G., Hawkins, A., and Popper, A. N. (**2014**). "International harmonization of approaches to define underwater noise exposure criteria," J. Acoust. Soc. Am. **135**, 2404.

MacGillivray, A. (**2018**). "Underwater noise from pile driving of conductor casing at a deep-water oil platform," J. Acoust. Soc. Am. **143**, 450–459.

MacGillivray, A. O. (**2014**). "A model for underwater sound levels generated by marine impact pile driving," Proc. Mtgs. Acoust. **20**, 045008.

Madsen, P. T., Wahlberg, M., Tougaard, J., Lucke, K., and Tyack, P. L. (**2006**). "Wind turbine underwater noise and marine mammals: Implications of current knowledge and data needs," Mar. Ecol. Prog. Ser. **309**, 279–295.

Martin, B., MacDonnell, J. T., MacGillivray, A. O., and Hannay, D. E. (**2016**). "Comparing methods for estimating the injury and behavioral disturbance radii from sound source characterization measurements," J. Acoust. Soc. Am. **139**, 2147–2148.

Matuschek, R., and Betke, K. (**2009**). "Measurements of construction noise during pile driving of offshore research platforms and wind farms," in *Proceedings of NAG-DAGA 2009 International Conference on Acoustics*, pp. 262–265.

National Marine Fisheries Service (U.S.) (NMFS) (**2016**). "Technical guidance for assessing the effects of anthropogenic sound on marine mammal hearing: Underwater acoustic thresholds for onset of permanent and temporary threshold shifts," NOAA Technical Memorandum NMFS-OPR-55 (U.S. Department of Commerce, National Oceanic and Atmospheric Administration, Silver Spring, MD), p. 178.

National Marine Fisheries Service (U.S.) (NMFS) (**2018**). "2018 revision to: Technical guidance for assessing the effects of anthropogenic sound on marine mammal hearing (version 2.0): Underwater thresholds for onset of permanent and temporary threshold shifts," NOAA Technical Memorandum NMFS-OPR-59 (U.S. Department of Commerce, National Oceanic and Atmospheric Administration, Silver Spring, MD), p. 167.

National Marine Fisheries Service (U.S.) (NMFS), and National Oceanic and Atmospheric Administration (U.S.) (NOAA) (**1995**). "Small takes of marine mammals incidental to specified activities; offshore seismic activities in southern California: Notice of issuance of an incidental harassment authorization," Fed. Regist. **60**, 53753–53760.

National Oceanic and Atmospheric Administration (U.S.) (NOAA) (**2012**). "Guidance document: Data collection methods to characterize impact and vibratory pile driving source levels relevant to marine mammals," Memorandum from NMFS Northwest Region and Northwest Fisheries Science Center (U.S. Department of Commerce, National Marine Fisheries Service, Seattle, WA),7 pp.

National Oceanic and Atmospheric Administration (U.S.) (NOAA) (**2013**). "Draft guidance for assessing the effects of anthropogenic sound on marine mammals: Acoustic threshold levels for onset of permanent and temporary threshold shifts," (National Oceanic and Atmospheric Administration, U.S. Department of Commerce, and NMFS Office of Protected Resources, Silver Spring, MD), p. 76.

National Oceanic and Atmospheric Administration (U.S.) (NOAA) (**2015**). "Draft guidance for assessing the effects of anthropogenic sound on marine mammal hearing: Underwater acoustic threshold levels for onset of permanent and temporary threshold shifts," (NMFS Office of Protected Resources, Silver Spring, MD), p. 180.

Newhall, A. E., Lin, Y. T., Miller, J. F., Potty, G. R., Vigness-Raposa, K., Frankel, A., Giard, J., Gallien, D. R., Elliot, J., and Mason, T. (**2016**). "Monitoring the acoustic effects of pile driving for the first offshore wind farm in the United States," J. Acoust. Soc. Am. **139**, 2181–2181.

Pinheiro, J., Bates, D., DebRoy, S., Sarkar, D., and R Core Team (**2017**). "nlme: Linear and nonlinear mixed effects models (R package version 3.1-131)," available at https://mran.microsoft.com/snapshot/2017-02-20/web/packages/nlme/index.html (Last accessed 23 June 2019).

Popper, A. N., Hawkins, A. D., Fay, R. R., Mann, D. A., Bartol, S., Carlson, T. J., Coombs, S., Ellison, W. T., Gentry, R. L., Halvorsen, M. B., Løkkeborg, S., Rogers, P. H., Southall, B. L., Zeddies, D. G., and Tavolga, W. N. (**2014**). "Sound exposure guidelines," in *Sound Exposure Guidelines for Fishes and Sea Turtles: A Technical Report Prepared by ANSI-Accredited Standards Committee S3/SC1 and registered with ANSI* (ASA S3/SC1.4 TR-2014), SpringerBriefs in Oceanography (ASA Press and Springer, New York).

Popper, A. N., Hawkins, A. D., and Halvorsen, M. B. (**2019**). "Anthropogenic sound and fishes," Report by ICF for Washington State Department of Transportation, Research Office, p. 170.

Reinhall, P. G., and Dahl, P. H. (**2011**). "An investigation of underwater sound propagation from pile driving," prepared for the State of Washington Department of Transportation, p. 39.

Robinson, S. P., Lepper, P. A., and Ablitt, J. (**2007**). "The measurement of the underwater radiated noise from marine piling including characterisation of a 'soft start' period," in *Oceans 2007-Europe* (IEEE, Aberdeen, UK), pp. 732–737.

Southall, B. L., Finneran, J. J., Reichmuth, C., Nachtigall, P. E., Ketten, D. R., Bowles, A. E., Ellison, W. T., Nowacek, D. P., and Tyack, P. L. (**2019**). "Marine mammal noise exposure criteria: Updated scientific recommendations for residual hearing effects," Aquat. Mamm. **45**, 125–232.

Tougaard, J., and Beedholm, K. (**2019**). "Practical implementation of auditory time and frequency weighting in marine bioacoustics," Appl. Acoust. **145**, 137–143.

Tougaard, J., Wright, A. J., and Madsen, P. T. (**2015**). "Cetacean noise criteria revisited in the light of proposed exposure limits for harbour porpoises," Mar. Pollut. Bull. **90**, 196–208.

Venables, W. N., and Ripley, B. D. (**2002**). *Modern Applied Statistics with S* (Springer, New York).

Wilkes, D. R., and Gavrilov, A. N. (**2017**). "Sound radiation from impact-driven raked piles," J. Acoust. Soc. Am. **142**, 1–11.

Zampolli, M., Nijhof, M. J. J., de Jong, C. A. F., Ainslie, M. A., Jansen, E. H. W., and Quesson, B. A. J. (**2013**). "Validation of finite element computations for the quantitative prediction of underwater noise from impact pile driving," J. Acoust. Soc. Am. **133**, 72–81.